GEOLOGICA CARPATHICA, OCTOBER 2010, 61, 5, 365–381 doi: 10.2478/v10096-010-0022-3

High resolution stratigraphy of the Jurassic-Cretaceous boundary interval in the Gresten Klippenbelt (Austria)

ALEXANDER LUKENEDER[1,*], EVA HALÁSOVÁ[2], ANDREAS KROH[1], SUSANNE MAYRHOFER[1], PETR PRUNER[3], DANIELA REHÁKOVÁ[2], PETR SCHNABL[3], MARIO SPROVIERI[4] and MICHAEL WAGREICH[5]

[1]Geological and Paleontological Department, Natural History Museum, Burgring 7, 1010 Vienna, Austria; *alexander.lukeneder@nhm-wien.ac.at
[2]Department of Geology and Paleontology, Faculty of Natural Sciences, Comenius University, Mlynská dolina G-1, 842 15 Bratislava, Slovak Republic; halasova@fns.uniba.sk; rehakova@fns.uniba.sk
[3]Institute of Geology, Academy of Sciences of the Czech Republic, v.v.i., Rozvojová 269, 165 00 Praha 6, Lysolaje, Czech Republic
[4]Institute for Marine and Coastal Environment (IAMC-CNR), Calata Porta di Massa (Interno Porto di Napoli), 80133 Napoli, Italy
[5]Department for Geodynamics and Sedimentology, Center for Earth Sciences, University of Vienna, Althanstrasse 14, 1090 Vienna, Austria

(Manuscript received February 8, 2010; accepted in revised form June 10, 2010)

Abstract: The key objective of investigation of hemipelagic sediments from the Gresten Klippenbelt (Blassenstein Formation, Ultrahelvetic paleogeographic realm) was to shed light on environmental changes around the Jurassic-Cretaceous (J/K) boundary on the northern margin of the Penninic Ocean. This boundary is well exposed in a newly discovered site at Nutzhof. Around the critical interval including the boundary, this new outcrop bears a rich microplanktonic assemblage characterized by typical J/K (Tithonian/Berriasian) boundary faunas. The Nutzhof section is located in the Gresten Klippenbelt (Lower Austria) tectonically wedged into the deep-water sediments of the Rhenodanubian Flysch Zone. In Late Jurassic–Early Cretaceous time the Penninic Ocean was a side tract of the proto-North Atlantic Oceanic System, intercalated between the European and the Austroalpine plates. Its opening started during the Early Jurassic, induced by sea floor spreading, followed by Jurassic–Early Cretaceous deepening of the depositional area of the Gresten Klippenbelt. These tectonically induced paleogeographic changes are mirrored in the lithology and microfauna that record a deepening of the depositional environment from Tithonian to Berriasian sediments of the Blassenstein Formation at Nutzhof. The main lithological change is observed in the Upper Tithonian *Crassicollaria* Zone, in Chron M20N, whereas the J/K boundary can be precisely fixed at the *Crassicollaria–Calpionella* boundary, within Chron M19n.2n. The lithological turnover of the deposition from more siliciclastic pelagic marl-limestone cycles into deep-water pelagic limestones is correlated with the deepening of the southern edge of the European continent at this time. Within the Gresten Klippenbelt Unit, this transition is reflected by the lithostratigraphic boundary between siliciclastic-bearing marl-limestone sedimentation in the uppermost Jurassic and lowermost Cretaceous limestone formation, both within the Blassenstein Formation. The cephalopod fauna (ammonites, belemnites, aptychi) and crinoids from the Blassenstein Formation, correlated with calcareous microfossil and nannofossil data combined with isotope and paleomagnetic data, indicate the Tithonian to middle Berriasian (*Hybonoticeras hybonotum* Zone up to the *Subthurmannia occitanica* Zone; M17r–M21r). The succession of the Nutzhof section thus represents deposition of a duration of approximately 7 Myr (ca. 150–143 Ma). The deposition of the limestone, marly limestone and marls in this interval occurred during tectonically unstable conditions reflected by common allodapic material. Along with the integrated biostratigraphic, geochemical and isotopic analysis, the susceptibility and gamma-ray measurements were powerful stratigraphic tools and important for the interpretation of the paleogeographic setting. Two reverse magneto-subzones, Kysuca and Brodno, were detected within magnetozones M20n and M19n, respectively.

Key words: Jurassic/Cretaceous boundary, Penninic Ocean, paleoecology, paleogeography, environmental changes.

Introduction

Jurassic and Lower Cretaceous pelagic sediments are known to form a major elements of the northernmost tectonic units of the Gresten Klippenbelt (Czjžek 1852; Kühn 1962; Küpper 1962; Gottschling 1965; Decker & Rögl 1988; Decker 1990; Piller et al. 2004). Preliminary results on a Jurassic-Cretaceous boundary section of the Gresten Klippenbelt were presented including description of new faunas and localities (Lukeneder 2009; Kroh & Lukeneder 2009; Pruner et al. 2009; Reháková et al. 2009).

The Gresten Klippenbelt at Nutzhof comprises Upper Jurassic (Tithonian) to Lower Cretaceous sediments belonging to the Blassenstein Formation. The lower part of the succession consists of marls, marly limestone and marl-limestone alternations, whereas the upper part of the Blassenstein Formation (Tithonian to Valanginian) is composed of very pure limestones. The biostratigraphy of the Lower Cretaceous sediments in the study area is mainly based on microfossils (Reháková et al. 2009). The first description of the lithology and stratigraphy of this area was provided by Czjžek (1852), followed by Küpper (1962). Biostratigraphic data on the Blassenstein Formation (Stollberger Schichten of Küpper 1962) near Nutzhof are remarkably scarce (Czjžek 1852; Küpper 1962).

The tectonically highly active northern zone of the Penninic Ocean (the southern margin of the European continent) is crucial for understanding the formation of the Penninic

Ocean, its subsequent subduction and the following Alpine history.

Formation of the Penninic Ocean, here defined to include the Ligurian Basin (sensu Dercourt et al. 1993, 2000; Masse et al. 2000; Mandic & Lukeneder 2008) and synonymous with the Alpine Tethys (Stampfli & Borel 2002 and Stampfli et al. 2002) was initiated in the Late Triassic by rifting and disjunction of the Austroalpine microcontinent from the southern European Plate margin (Stampfli & Mosar 1999; Scotese 2001). It formed an eastern prolongation of the North Atlantic Rift-System, which affected the final break-up of the Permo-Triassic supercontinent Pangaea (e.g. Faupl 2003). The formation of the oceanic crust and the sea-floor spreading lasted from the Middle Jurassic to the Early Cretaceous, terminating with the introduction of its southward-directed subduction beneath the northern Austroalpine plate margin (Faupl & Wagreich 2000; Mandic & Lukeneder 2008). This tectonic phase is reflected by the lithological change within the Nutzhof section. An increasing deepening, reflected in the sedimentary succession (e.g. allodapic limestones and microturbidites), in the section at Nutzhof, marks the opening of the Penninic Ocean. The pelagic carbonate sedimentation, which started in the Late Jurassic, changes from siliciclastic-dominated limestone deposition to pure limestone-dominated. The Penninic Ocean persisted from the Late Jurassic until close to the end of the Cretaceous.

The paleomagnetic and rock-magnetic study is a continuation of detailed paleontological and magnetostratigraphic studies of the Jurassic/Cretaceous (J/K) boundary in the Tethyan Realm (Houša et al. 1999). The section at Brodno near Žilina, W Slovakia, was the first section investigated with high-resolution magnetostratigraphy and micropaleontology in the Carpathians (Houša et al. 1999). Magnetostratigraphic studies were carried out in the Bosso Valley of Umbria, Italy (Houša et al. 2004) and the Tatra Mountains, Poland (Grabowski & Pszczółkowski 2006). The magnetostratigraphic investigations published by Pruner et al. (2009) preliminarily determine the boundaries of magnetozones M17n to M22r (six reverse and six normal zones). The aim of these studies was to globally and objectively establish a correlation between biozones around the J/K boundary in the Tethyan Realm using global paleomagnetic events and precisely determine the boundaries of magnetozones M19 and M20 including narrow reverse subzones. These studies provided a precise record of polarity changes in the Earth's magnetic field and determined their stratigraphic positions precisely within a biochronostratigraphic zonation.

The Nutzhof locality represents the only known section that includes the J/K boundary interval in the Gresten Klippenbelt. The section contains rich assemblages of radiolarians, calpionellids, saccocomids, nannofossils and in some intervals ammonites. The J/K boundary sediments of the Nutzhof section provide an excellent succession for quantitative and integrated methods due to their fossiliferous and undisturbed bedding for a period of almost 7 million years.

Location and geological setting of Nutzhof

Locality description

The Nutzhof locality is situated in the Gresten Klippenbelt of Lower Austria (48°04′49″ N, 15°47′36″ E), about 20 km south of Böheimkirchen and 5 km north of Hainfeld (Fig. 1), 600 m above sea level (m a.s.l.) (ÖK 1:50,000, sheet 56 St. Pölten). The outcrop is located in an abandoned quarry in the south-eastern-most part of the northeast-southwest striking Gresten Klippenbelt, between Kasberg (785 m a.s.l.) to the east and the vicinity of the Nutzhof (550 m a.s.l.) to the west. The quarry is located on the northern side of the Kasberg ridge and the measured section is exposed on the eastern side of the quarry.

Geological setting

The Gresten Klippenbelt at Nutzhof is surrounded by deep-water successions of the Rhenodanubian Flysch Zone. The Gresten Klippenbelt represents an independent and scarcely known geological unit. It is tectonically incorporated in the Flysch Zone as a long, thin, east-west striking marly and calcareous unit (Fig. 1). Sediments from the Gresten Klippenbelt are considered to belong to the southern part of the Helvetic paleogeographic realm. The Gresten Klippenbelt sediments were deposited on the southern shelf and

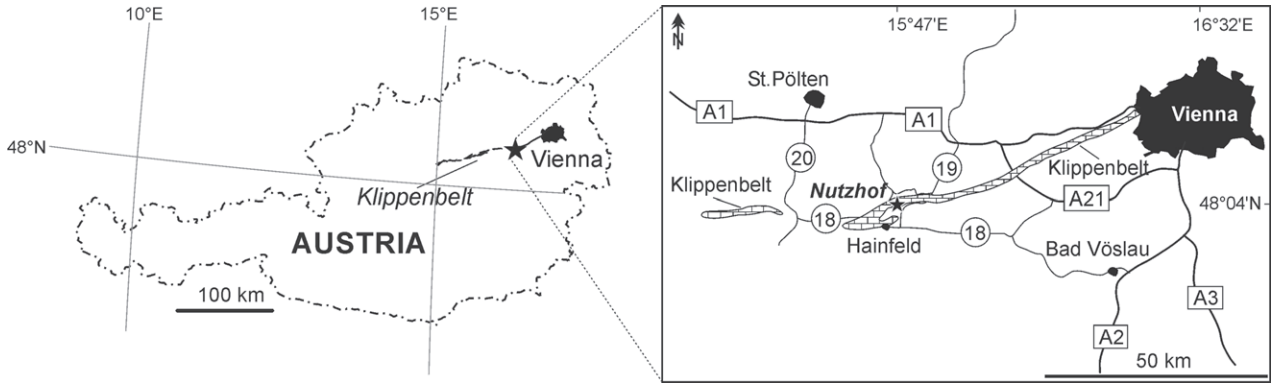

Fig. 1. Locality map of Austria with indicated position of the Nutzhof locality in Lower Austria (left). Detailed map of the area around Nutzhof with outcrop position within the Jurassic–Cretaceous Klippenbelt (right).

slope of the European continent, on the slope of the Bohemian Massif at the north-western margin of the Penninic Ocean. The Nutzhof site consists of two different facies within the Blassenstein Formation (Lukeneder 2009). The lower part (Tithonian; 18.0–10.0 m) with dark marl-limestone alternations and its characteristically intercalated limestone beds, and the upper part (Tithonian–Berriasian; 10.0–0.0 m) with light grey, almost pure limestone. Limestone beds display uniform overturned bedding-plane orientation. The mean strike is 151°±30° and the mean dip angle 44°±22°. The succession is characterized by a marked lithological and faunal change at Nu 10.0 which does not coincide with the Jurassic/Cretaceous boundary at bed Nu 7.0 (Nu for Nutzhof samples). Sediments occur as wacke-, pack- or mudstones.

The Nutzhof section

The Jurassic-Cretaceous boundary in the Gresten Klippenbelt

The most recent reports concerning the J/K boundary interval from the Gresten Klippenbelt present preliminary results (Lukeneder 2009; Kroh & Lukeneder 2009; Pruner & al. 2009; Reháková et al. 2009) (Fig. 2). Therein first results have been presented on macro-, micro- and nannofossils. Tectonic units including the J/K boundary of the Gresten Klippenbelt were reported by Cžjžek (1852), Kühn (1962), Küpper (1962), Gottschling (1965), Decker & Rögl (1988), Decker (1990) and Piller et al. (2004).

Materials and methods

The Jurassic-Cretaceous boundary section at Nutzhof was studied with an integrated approach. Beds were sampled for biostratigraphical, paleomagnetic, geochemical ($CaCO_3$, TOC, S) and istotopic ($\delta^{18}O$, $\delta^{13}C$, $\delta^{87}Sr$) data. Focus is directed to an interval of about 18.0 m (Nu 0.0–Nu 18.0) that was studied in detail (Figs. 2, 3, 4). Macro-, micro- and nannofossil contents were quantitatively investigated (Fig. 4). Samples were collected at intervals of 0.1 and 0.2 meters for stable isotopes, total organic carbon (TOC), sulphur (S), calcium carbonate ($CaCO_3$), susceptibility and gamma log. The microfossil content was analysed for calpionellids, radiolarians, saccocomids (thin sections) and insoluble residues. High resolution studies were combined with grey-scale quantification, gamma-ray and susceptibility analyses. Sample numbers, for example Nu 10.0, correspond to the sample interval at 10.0 m within the log (for all numbers and figures, Nu = Nutzhof). All samples are stored at the Natural History Museum of Vienna, in the collection of the Department of Geology and Paleontology.

Gamma-ray analysis

The gamma log measures the radioactivity of the rock, which represents a direct function of its clay-mineral content. Increasing radioactivity reflects the increasing clay content. Gamma response (counts per second — cps) was measured using a hand-held standard gamma-ray scintillometer.

Macrofossils

Macrofossil material includes 46 ammonite specimens, 238 lamellaptychi and 82 rhyncholites were examined. Four brachiopods and three inoceramids as well as a single belemnite specimen were collected. Ammonites are preserved as steinkerns or are represented by calcitic aptychi. Shell-preservation is restricted to organisms with primary skeletal calcite of belemnite-rostra and brachiopods in addition to rare inoceramid fragments (calcitic prisms). The ammonite assemblage contains six different genera: *Subplanites*, *Haploceras*, *Phylloceras*, *Ptychophylloceras*, *Lytoceras* and *Leptotetragonites* dominated by the perisphinctid genus *Subplanites* (Lukeneder 2009).

Calpionellids and calcareous nannofossils

Quantitative micro- and nannofacies analysis includes study of calpionellids and calcareous dinoflagellates in 93 thin sections. The thin sections are deposited in the Natural History Museum in Vienna; NHMW 2007z0271/0000. Changes in the distribution of calpionellids and calcareous nannofossils were studied in detail in order to correlate them with the changes in nannoplankton associations (Figs. 2, 3 and 4).

Calcareous nannofossils were analysed semiquantitatively in 19 smear slides, prepared from all lithologies by standard techniques, using a light polarizing microscope at 1250× magnification. At least 200 specimens were counted in each slide to record relative abundances and the stratigraphic range of taxa (Figs. 2, 3). Nannofossil preservation can be characterized as moderately to intensely etched by dissolution. The calcareous nannofossil zones were adopted from the zonal scheme proposed by Bralower et al. (1989).

Magnetic components

Paleomagnetic analyses presented in this studies come from 244 samples, but the preliminary results include only 111 samples (see Pruner et al. 2009). All the samples were subjected to progressive thermal demagnetization (TD) or alternating field (AF) demagnetization in 11–12 temperatures or fields. The individual components were precisely established using multicomponent analysis of remanence (Kirschvink 1980). Isothermal remanent magnetization (IRM) to saturation was measured to identify magnetically active minerals. Magnetomineralogical analyses and unblocking temperature determination show that magnetite and goethite are the main carriers of remanent magnetization.

Microfossils

Apart from thin sectioning also employed for a study of calpionellids, an effort was made to obtain three-dimensional specimens of the crinoids and other microfossils commonly observed in the thin sections (namely foraminifers, ostracods, rhyncholites, small aptychi, ophiuroid remains,

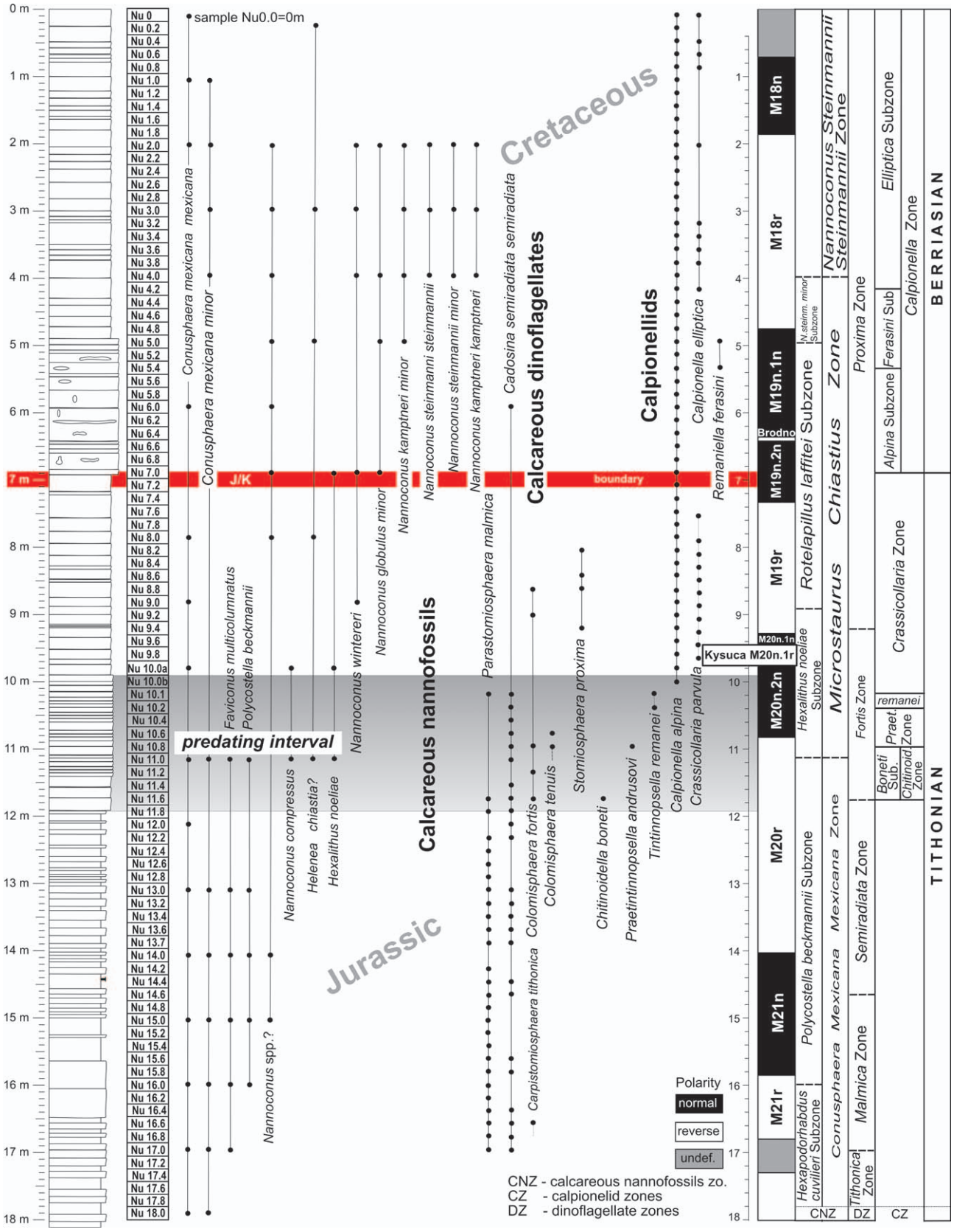

Fig. 2. Nutzhof log with occurrence and range of calcareous nannofossils, calcareous dinoflagellates and calpionellids and indicated paleomagnetic zonation: normal magnetozones are denoted black, reverse zones in white, and unknown parts in grey.

etc.). Bulk samples were collected in closely spaced intervals in the lower, marly part of the succession (10.0–18.0 m). Strong lithification hampered dense bulk sampling in the upper part of the section (0 to 10.0 m). These beds were analysed by thin sections only. Traditional washing methods were not applicable due to strong lithification of the sediment. Partial disaggregation was achieved by repetitive, combined treatment with hydrogen-superoxide and the tenside Rewoquat (see Lierl 1992). After cleaning, the microfossils were hand picked under a microscope. For the present study we used the sediment fractions larger than 250 μm only.

TC and TOC content

Calcium carbonate contents ($CaCO_3$; wt. % bulk rock, TC) were determined using the carbonate bomb technique. Total carbon content was determined using a LECO WR-12 analyser. Total organic carbon (TOC) contents were calculated as the difference between total carbon and carbonate carbon, assuming that all carbonate is pure calcite. All the chemical analyses were carried out in the laboratories of the Department of Forest Ecology at the University of Vienna.

Stable isotopes

A total of 37 bulk sample stable isotope analyses were measured by automated continuous flow carbonate preparation GasBenchII device (Spötl & Vennemann 2003) and ThermoElectron Delta Plus XP mass spectrometer at the IAMC-CNR (Naples) isotope geochemistry laboratory. Acidification of samples was performed at 50 °C. For each six samples, an internal standard (Carrara Marble with $\delta^{18}O = -2.43$ vs. V-PDB and $\delta^{13}C = 2.43$ vs. V-PDB) was run, and for each 30 samples, the NBS19 international standard was measured. Standard deviations of carbon and oxygen isotope measures were estimated 0.1 and 0.08 ‰, respectively, on the basis of ~10 repeated samples.

All the isotope data are reported in per mil (‰) relative to the V-PDB standard.

$^{87}Sr/^{86}Sr$ isotope data were analysed from 19 bulk-rock samples of limestones at the Geochronological Laboratory of the Department of Lithospheric Research, Centre for Earth Sciences, University of Vienna using strontium separation by standard methods of ion-exchange chromatography and isotope ratio measurements on a TIMS (Triton mass spectrometer). The measured NBS 987 standard value during measurements was 0.710256+/–0.000004 (7 measurements) and samples were not adjusted to the NBS 987 standard value of 0.710248.

Data and results

Biostratigraphy and magnetostratigraphy

The stratigraphic investigation of the calcareous microfossils (calpionellids, calcareous dinoflagellates) and nannofossils demonstrate that the Nutzhof section represent the Lower Tithonian–middle Berriasian. The calcareous dinoflagellate cyst zonation of Reháková (2000a) was followed. The presence of the Lower Tithonian *Tithonica*, *Malmica* and *Semiradiata* cyst Zones is demonstrated. The standard calpionellid zones and subzones proposed by Reháková (1995) and Reháková & Michalík (1997) were adopted for the biostratigraphic subdivision of the section into the *Chitinoidella* Zone (*Boneti* Subzone), the *Praetintinnopsella* Zone and the *Crassicollaria* Zone (*Remanei* Subzone). These belong to the middle to Upper Tithonian. The standard *Calpionella* Zone (*Alpina*, *Ferasini* and *Elliptica* Subzones) were observed in the overlying Lower Cretaceous (Fig. 2).

The nannofossil zones include the *Conusphaera mexicana mexicana* Zone, *Microstaurus chiastus* and *Nannoconus steinmannii steinmannii* Zones. This stratigraphic interval corresponds to the Lower Tithonian *Hybonoticeras hybonotum* ammonite Zone to the middle Berriasian *Subthurmannia occitanica* ammonite Zone, demonstrated in the Nutzhof section on chronostratigraphic diagnostic cephalopods (*Subplanites fasciculatiformis*, *Ptychophylloceras ptychoicum*, *Leptotetragonites honnoratianus*, *Haploceras elimatum*, *Hibolithes* (gr.) *semisulcatus* and some lamellaptychi.

The magnetostratigraphic log across the Nutzhof section includes the M21r to the M17r magnetozones subdivided into the Kysuca (M20r) and Brodno (M19r) subzones (Figs. 2, 6). The average sedimentation rate in the Nutzhof section is ca. 3.7 m/Myr (Fig. 7), but with high dispersion (from 2–11 m/Myr). The scatter of the sedimentation rate is similar to Hlboča profile in Slovakia (Grabowski et al. 2010). The main difference between these two sections is in the thickness of M19 and M20 mangentozones. Nutzhof has higher sedimentation rate at M19 while Hlboča appears with higher rates in M20.

Macrofossil content

The macrofossil content is characterized by ammonoids, aptychi, belemnites, brachiopods, bivalves and echinoderms. The ammonite fauna comprises six different genera represented by *Lytoceras sutile* Oppel, *Lytoceras* sp., *Leptotetragonites honnoratianus* (d'Orbigny), *Phylloceras* sp., *Ptychophylloceras ptychoicum* (Quenstedt), *Haploceras* (*Haploceras*) *elimatum* (Oppel), *Subplanites fasciculatiformis* Lukeneder. The ammonite fauna is dominated by the perisphinctid-type. Ammonitina is the most common component (60 %; *Subplanites* and *Haploceras*), followed by the Phylloceratina (25 %; *Ptychophylloceras* and *Phylloceras*), and the Lytoceratina (15 %; represented by *Lytoceras* and *Leptotetragonites*). The belemnite *Hibolithes* (gr.) *semisulcatus* (Münster) and aptychi (*Lamellaptychus*) occur. Only Mediterranean cephalopod elements are present at Nutzhof. Brachiopods are represented by *Triangope*, bivalves by inoceramid shells and echinoderms by crinoids (*Phyllocrinus belbekensis* Arendt, *Balanocrinus* sp., *Crassicoma*? sp. and *Saccocoma tenella* (Goldfuss).

The crinoid fauna recovered from the bulk samples of Nutzhof is typical for Upper Jurassic strata of Central and Eastern Europe. The low diversity of stalked crinoids, common in many contemporaneous deposits (Hess et al. 1999), may be interpreted as a result of the distal position of the sec-

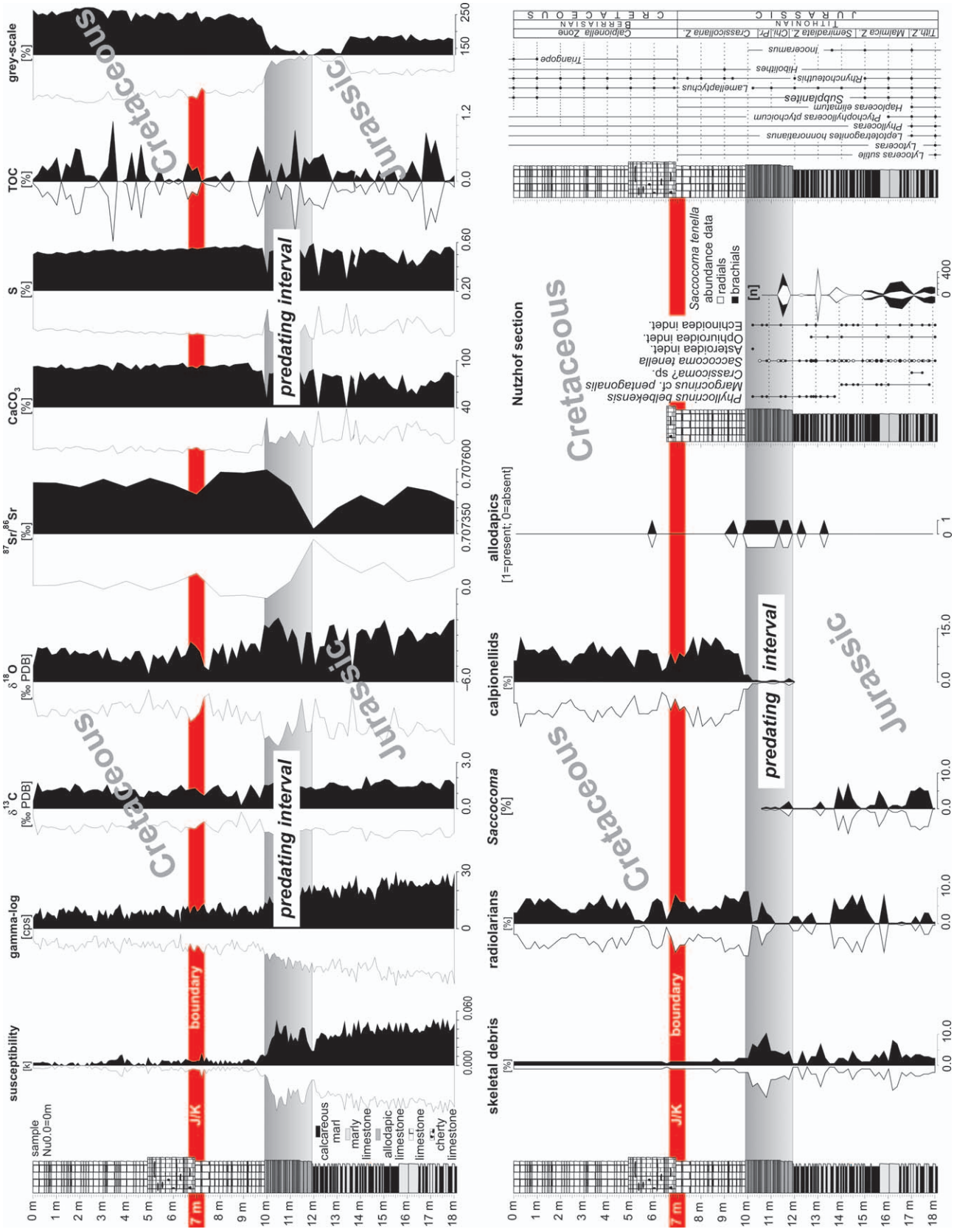

Fig. 3. Compiled geochemical, isotope and fossil data on the J/K boundary at Nutzhof. Note the change at the predating interval at meter 7 below the J/K boundary.

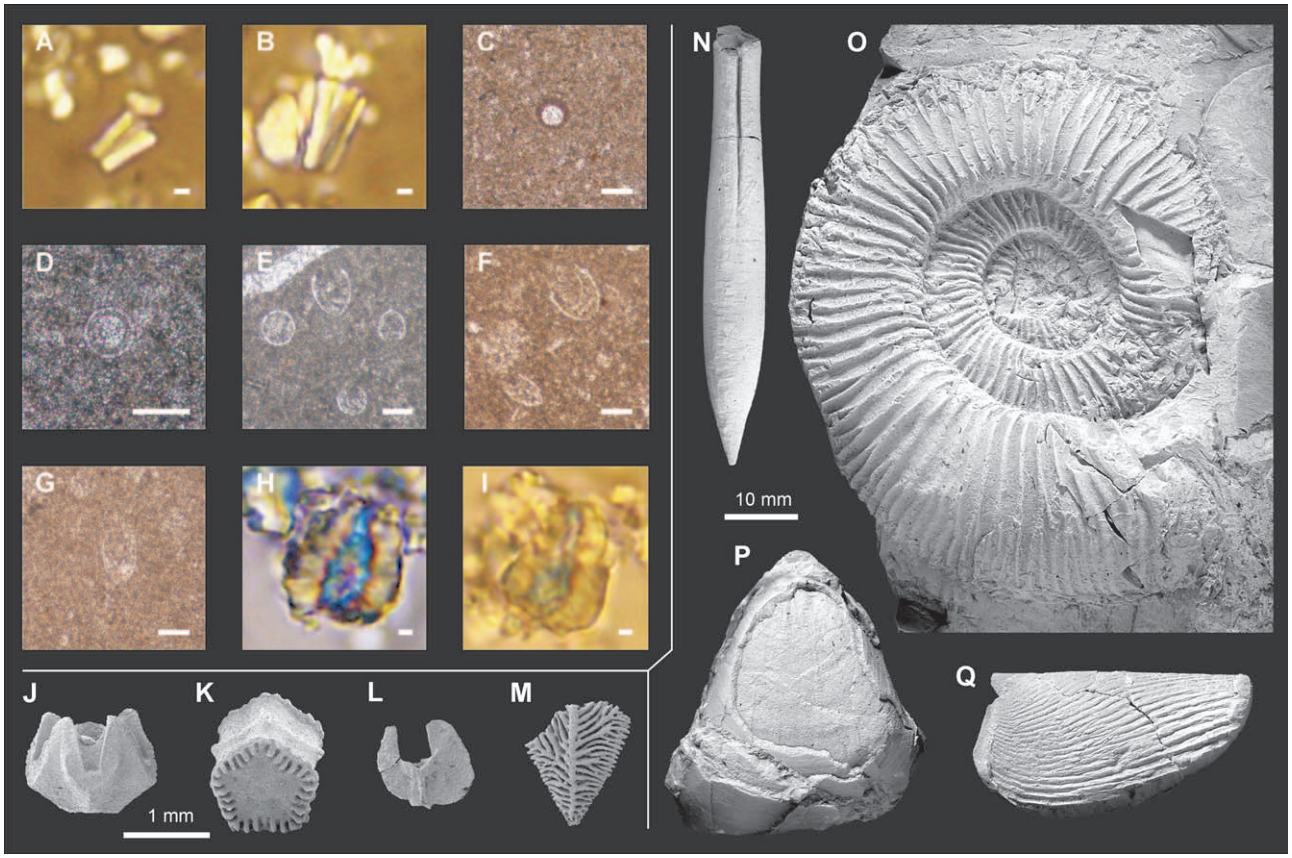

Fig. 4. A — *Conusphaera mexicana minor* Bown & Cooper; Nu 18.0, NHMW2008z0271/0028. **B** — *Conusphaera mexicana mexicana* Bralower et al.; Nu 17.0, NHMW2008z0271/0003. **C** — *Cadosina semiradiata semiradiata* Wanner; 17.0, NHMW2008z0271/0003. **D** — *Parastomiosphaera malmica* (Borza); Nu 13.0, NHMW2008z0271/0002. **E** — *Calpionella alpina* Lorenz and *Calpionella grandalpina* Nagy; Nu 9.8, NHMW2008z0271/0011. **F** — *Crassicollaria parvula* Remane and *Calpionella grandalpina*; Nu 9.6, NHMW2008z0271/0012. **G** — *Calpionella elliptica* Cadisch; Nu 3.2, NHMW2008z0271/0014. **H** — *Nannoconus steinmannii steinmannii* Kamptner; Nu 4.0, NHMW2008z0271/0034. **I** — *Nannoconus kamptneri kamptneri* Brönnimann; Nu 2.0, NHMW2008z0271/0035. **J** — *Phyllocrinus belbekensis* Arendt; Nu 12.3; NHMW 2008z0226/001. **K** — *Balanocrinus* sp.; Nu 14.6, NHMW2008z0228/0003. **L** — *Saccocoma tenella* (Goldfuss); Nu 11.5, NHMW2008z0236/0015. **M** — *Saccocoma tenella* (Goldfuss); Nu 13.0, NHMW2008z0236/0012. **N** — *Hibolithes* (gr.) *semisulcatus* (Münster); Nu 14.3, NHMW2008z0264/0025. **O** — *Subplanites fasciculatiformis* Lukeneder; Nu 17.0, NHMW2008z0264/0012. **P** — *Triangope* sp.; Nu 1.0, NHMW2008z0264/0028. **Q** — *Lamellaptychus* sp.; Nu 18.0, NHMW2008z0264/0024. Graphic scale bars equal 1 μm for A, B and H, I; 50 μm for C–G; 1 mm for J–K, and 10 mm for N–Q.

tion, which represents a deep-water facies. The incomplete size ranges of isocrinid and phyllocrinid ossicles, the lack of fragile elements and the presence of allodapic material (Lukeneder 2009) suggest that the majority of the crinoid material is allochthonously deposited. Saccocomid fragments, in contrast, are not sorted and include abundant fragile elements suggesting that these crinoids are autochthonous.

Of the crinoid material only the saccocomids can be used for biostratigraphy. *Saccocoma tenella* is restricted to the Upper Kimmeridgian–Upper Tithonian. From a biogeographic point of view the faunal composition indicates connections with contemporaneous units of the northern Tethys shelf in Eastern Europe.

Microfacies and calcareous microplankton assemblages

The limestones in the section include wackestones, packstones and mudstones. Fine-grained micrite with pelagic microfossils (calpionellids, calcareous dinoflagellates, radiolarians) and calcareous nannofossils characterize an open-marine environments. Rare skeletal debris from fragmented and disintegrated shells of invertebrates (benthic foraminifers, echinoderms, molluscs) are derived from shallower environments. The studied microfacies are typical for basinal settings.

Calpionellids

Calpionellids in the studied samples are generally well-preserved. Hyaline forms dominate, whereas chitinoidellids are rare. The chitinoidellid taxonomy of Pop (1997) and Reháková (2002) is followed here. The group is represented by *Borziella slovenica* (Borza), *Dobeniella tithonica* (Borza) and *Chitinoidella boneti* Doben, species typical for the *Boneti* Subzone of the *Chitinoidella* Zone (Figs. 2, 4). The appearance of first hyaline calpionellid loricas of *Praetintinnopsella andrusovi* Borza and *Tintinnopsella remanei* Borza

precede the crassicollarian radiation. *Crassicollaria parvula* Remane and *Calpionella alpina* Lorenz dominate relative to *Crassicollaria massutiniana* (Colom), *Calpionella grandalpina* Nagy and *Tintinnopsella carpathica* (Murgeanu & Filipescu) in the *Remanei* Subzone of the *Crassicollaria* Zone. Higher in the section, crassicollarians abruptly decrease in abundance, being replaced by an interval with radiation of small spherical forms of *Calpionella alpina* Lorenz. The diversification of a monospecific calpionellid association started in the overlying *Ferasini* and *Elliptica* Subzones of the standard *Calpionella* Zone where *Calpionella alpina* Lorenz is accompanied by *Tintinnopsella carpathica* (Murgeanu & Filipescu), *Remaniella ferasini* Pop, *R. duranddelgai* Pop, *R. catalanoi* Pop, *Calpionella elliptica* (Cadisch), *Tintinnopsella longa* (Colom), and *Lorenziella hungarica* Knauer.

Calcareous dinoflagellates

Calcareous dinoflagellates predominate in the Lower and Upper Tithonian being represented by *Cadosina parvula* Nagy, *Carpistomiosphaera borzai* (Nagy), *Schizosphaerella minutissima* (Colom), *Parastomiosphaera malmica* (Borza), *Cadosina semiradiata semiradiata* Wanner, *Cadosina semiradiata fusca* (Wanner), *Carpistomiosphaera tithonica* Nowak, *Colomisphaera fortis* Řehánek, *Colomisphaera tenuis* (Nagy), *Colomisphaera carpathica* (Borza), and *Stomiosphaerina proxima* Řehánek. For the first time the appearance of *Colomisphaera fortis* Řehánek precedes the appearance of *Colomisphaera tenuis* (Nagy), hampering the determination of the *Tenuis* and *Fortis* dinoflagellate Zones sensu Řehánek (1992) (Figs. 2, 4).

Calcareous nannofossils

The semiquantitative study (Figs. 2, 3) reveals that only the taxa *Conusphaera* spp., *Polycostella* spp., *Nannoconus* spp., *Cyclagelosphaera margerelii* Noël, *Watznaueria barnesae* (Black) Perch-Nielsen, and *W. manivitae* Bukry occur in significant abundances. Nannofossils indicative of eutrophic environments such as *Zeugrhabdotus erectus* (Deflandre) Reinhardt, *Diazomatholithus lehmannii* Noël, and *Discorhabdus ignotus* (Górka) Perch-Nielsen occur sporadically.

The calcareous nannofossil assemblage from the basal part of the Nutzhof section (samples 17, 18, *Tithonica* dinoflagellate Zone) contains the dissolution-resistant nannofossil species *Conusphaera mexicana mexicana* Bralower et al., *Conusphaera mexicana minor* Bown & Cooper, *Cyclagelosphaera margerelii*, *Cyclagelosphaera deflandrei* (Manivit) Roth, *Watznaueria barnesae*, *Watznaueria britannica* (Stradner) Reinhardt, and *Watznaueria manivitae*. The FO (first occurrence datum) of *Faviconus multicolumnatus* Bralower was recorded. The absence of the nannolith *Polycostella beckmannii* Thierstein allowed us to distinguish the *Conusphaera mexicana mexicana* NJ20 Zone; *Hexapodorhabdus cuvillieri* Subzone NJ20-A (Roth et al. 1983; emended Bralower et al. 1989) of the Lower Tithonian.

The calcareous nannofossil assemblages from the samples Nu 16.0 to Nu 12.0 show dominance of *Watznaueria* and *Conusphaera*. The FOs of *Zeugrhabdotus embergeri* (Noël) Perch-Nielsen, *Zeugrhabdotus erectus*, and *Diazomatholithus lehmannii* were observed. The FO of the nannolith *Polycostella beckmannii* is the most significant marker indicating the base of the *Polycostella beckmannii* Subzone NJ20-B of the *Conusphaera mexicana mexicana* Zone, NJ20 (Roth et al. 1983; emended Bralower et al. 1989). The age of this Subzone is middle Tithonian. The range of the *Polycostella beckmannii* Subzone NJ20-B fits with dinoflagellate *Malmica* and *Semiradiata* Zones and the lower part of the *Chitinoidella* Zone.

The calcareous nannofossils investigated in sample Nu 11 reflect a rather distinct change. The FO of *Helenea chiastia* Worsley, *Hexalithus noeliae* Loeblich & Tappan and the nannolith species *Nannoconus compressus* Bralower et al. are evidence for the base of the *Microstaurus chiastius* Zone NJK Bralower et al., 1989 and its *Hexalithus noeliae* Subzone NJK-A, which is thought to represent the Late Tithonian interval. The Subzone coincides with the upper part of the *Chitinoidella* Zone.

The calcareous nannofossil assemblages from samples Nu 9.0 to Nu 6.0 contain dissolution-resistant nannofossil genera *Conusphaera*, *Cyclagelosphaera*, *Watznaueria*, *Diazomatholithus* and *Assipetra*. The FAD of *Nannoconus wintereri* Bralower & Thierstein (1989) was observed (sample 9.0). Many remains of dissolution-susceptible coccoliths are present. In the upper part of the studied interval, the abundance of *Conusphaera* drops. This interval was correlated with the *Microstaurus chiastius* Zone NJK, Subzone *Rotelapillus laffitei* NJK-C, determining the J/K boundary interval. It shows good correlation with the upper part of the Upper Tithonian *Crassicollaria* Zone and the *Calpionella* Zone (*Alpina* Subzone), which represent the J/K boundary interval.

The interval bearing the calpionellid species of the Lower Berriasian *Calpionella* Zone (*Ferasini* Subzone) (sample Nu 5.0) shows a distinctive change in the calcareous nannofossil assemblage — the onset of nannoconids (*Nannoconus globulus minor* Bralower, *Nannoconus steinmannii minor* Deres & Achéritéquy, *Nannoconus kamptneri minor* Bralower, *Nannoconus cornuta* Deres & Achéritéquy). This nannofossil event indicates the base of the *Nannoconus steinmannii minor* Subzone NJK-D (*Microstaurus chiastius* Zone NJK) Bralower et al., which belongs to the lowermost Berriasian.

The calcareous nannofossils studied from the sample interval Nu 4.0–Nu 0.0 (correlating with the calpionellid *Calpionella* Zone, *Elliptica* Subzone) record the diversification of nannoconids. The FAD of *Nannoconus steinmannii steinmannii* Kamptner is recorded at level Nu 2.0. It could reflect the explosion in nannoconid abundance (sensu Bralower et al. 1989: p. 188). *Nannoconus globulus minor, Nannoconus kamptneri minor*, *Nannoconus wintereri*, *Nannoconus globulus globulus* Deres & Achéritéquy, *Nannoconus steinmannii minor* Deres & Achéritéquy, *Nannoconus steinmannii steinmannii*, and *Nannoconus kamptneri kamptneri* Brönnimann, *Nannoconus* spp. indicative of the *Nannoconus steinmannii steinmannii* Zone NK-1, Bralower et al. (1989), which is middle Berriasian in age.

On the basis of calcareous nannofossil distribution, the interval between the FO of *Nannoconus wintereri* co-occurring with small nannoconids in bed Nu 9.0 and the FO of *Nanno-*

conus steinmannii minor in bed Nu 5.0 (FAD after Hardenbol et al. 1998 — 143.92 Ma) is interpreted as the Tithonian-Berriasian boundary interval (Figs. 2, 3).

Stable isotope data

Oxygen and carbon (O, C)

The bulk carbon-isotope values (Fig. 3) lie between +0.49 and +2.10 ‰ corresponding to biogenic calcite precipitated under open marine conditions during the Jurassic–Cretaceous (e.g. Weissert et al. 1985). All $\delta^{18}O$ values are between –1.94 to –5.49 ‰ and appear depleted relative to diagenetically unaltered marine calcite (e.g. van de Schootbrugge et al. 2000, and reference therein). This reflects elevated temperature during burial diagenesis and/or effects of meteoric diagenesis (Weissert 1989). The carbon isotope signal is considered of primary importance as a calibration tool between ammonites and magnetostratigraphy (Hennig et al. 1999), but it should be noted that the absence of covariance between $\delta^{18}O$ and $\delta^{13}C$ suggests a limited influence of secondary diagenesis on the isotope record (Fig. 3).

A positive trend in the $\delta^{13}C$, from the base of the section at Nu 18.0 up to Nu 14.0, is followed by a decreasing excursion shifting the isotope values to their lowest values (0.69 ‰) at about Nu 10.0. After that point the $\delta^{13}C$ values stabilize at near constant averages of ~1.20 ‰.

Strontium (Sr)

$^{87}Sr/^{86}Sr$ isotope data from the section show a range from 0.707370 +/–0.000004 to 0.707598 +/–0.000004. A gentle trend from lower values in the lower, Jurassic part of the section (Nu 18.0–Nu 12.0: mean 0.707472) to higher values in the upper part including the J/K boundary and the Cretaceous interval (Nu 11.0–Nu 0.0: mean 0.707553) can be recognized (Fig. 3). A special interval is represented in the strong increase from Nu 13.0 (lowest isotope value) to Nu 11.0 (highest isotope value) and probably indicate a local diagenetic phenomenon. The slight increase of mean strontium isotope ratios in the section is compatible with the general increase of strontium isotope ratios from the latest Jurassic into the earliest Cretaceous as reported by the strontium isotope seawater curve of McArthur et al. (2001) and McArthur & Howarth (2004). The values measured in the present study are generally higher by a factor of ca. 0.0002 compared to the values reported by McArthur & Howarth (2004), who measured Upper Tithonian values around 0.707150 and Berriasian values between 0.707200–0.70725 (see also McArthur et al. 2007) with the Berriasian/Valanginian boundary slightly above 0.707300. Thus, the lowest measured value in the Nutzhof section thus does not fall within the J/K boundary range of values recorded by McArthur & Howarth (2004). This confirms a strong diagenetic overprint upon strontium isotope values. However, the increase in mean values is within the reported magnitude of increase expected for the J/K boundary interval, thus being compatible with the stratigraphy inferred by other methods, but precluding detailed dating.

Geochemistry

The $CaCO_3$ (calcium carbonate contents, equivalents calculated from total inorganic carbon; carbonate bomb) differ markedly in the lower and upper part of the log. The lower part shows variations from 89.03 % (Nu 12.0) in limestone beds to 40.72 % (Nu 13.4) in marl beds, whereas the upper part displays more constant values ranging from 86.16 % (Nu 9.6) up to the highest measured value of 97.4 % (Nu 3.6).

As recorded by the biostratigraphic results, the strong lithological and faunal changes at Nu 12.00 and Nu 10.0 are 3 to 5 meters below the Jurassic/Cretaceous boundary (Bed Nu 7.0) indicating changes in depositional environment 0.5 to 1 million years before the end of the Jurassic. The interval from Nu 12.0–10.0 ($CaCO_3$ 89.03–68.97 %; S 0.59–0.45 %; TOC up to 0.97 %) differs markedly and heralds the environmental change observed (Fig. 3).

Both the $CaCO_3$ and the S content clearly show a trend towards higher values and stable conditions from bed Nu 10.00 to Nu 18.00. Unstable conditions are mirrored in alternating values in the lower part of the log by variations from 89.03 % $CaCO_3$ and 0.59 % S (Nu 12.0) in limestone beds to 40.72 % and 0.30 % (Nu 13.4) in marl beds.

The range is smaller and more constant in the interval Nu 10.0–18.0 with $CaCO_3$ values from 86.16 % at Nu 9.6 up to the maximum value of 97.4 % at Nu 3.6. The total sulphur content is positively correlated to the $CaCO_3$ values. The maximum value is at bed Nu 9.0 with 0.58 % S and its minimum with 0.5 % S in bed Nu 0.0. As confirmed by Hirano (1993) the sulphur content is a reliable index for oxic-anoxic conditions of the bottom water and sediment at the time of preservation.

The weight % TOC values show no positive correlation with S or $CaCO_3$. TOC values oscillate throughout the log. They vary from 0.001 % to 0.91 % (Nu 11.2) in the lower part and from 1.07 % (Nu 3.4) to 0.001 % in the upper part.

The above described geochemistry is also reflected in the results of grey-scale data marking siliciclastic input. The section can be subdivided into three parts: a lower part (Nu 18.0–12.0) with 170–111 (mean 140.5), a middle part (Nu 12.0–10.0) with 138–90 (mean 114) and an upper part (Nu 10.0–0.0) with 254–195 (mean 224.5). In combination with other analyses, the grey-scale factor is a good indicator for siliciclastic input (clay, not sandstone) in pelagic to hemipelagic sediments. This indicates the dominance of siliciclastic components and allodapic microturbidites within the dark mid-part. These results corroborate those obtained from susceptibility and gamma log (increasing values show higher contents in clay minerals), thin sectioning and microfacies analysis.

Susceptibility

Susceptibility measurements at Nutzhof represent a direct function of the clastic or turbiditic content and associated mineral spectra (Fig. 3). Higher susceptibility data reflect higher detritic input of terrigenous material. The paleomagnetic data given in the magnetostratigraphic profile indicate a significant jump of remanent magnetization and magnetic

susceptibility, at Nu 10.0. This change marks the change from marls and marly limestone to pure limestone. Magnetosusceptibility measurements allow a subdivision of the Nutzhof section into three parts or intervals. A general decreasing trend throughout the log reflects a decreasing content of siliciclastic material indicating a decrease in clastic input to the depositional area at Nutzhof during the Late Jurassic–Early Cretaceous. Mean values of volume magnetic susceptibility (k) are shown in Table 1. The k ranges from –8.6 to 15.6×10^{-6} SI for upper interval between 0–10 m of the section and from 30 to 85.1×10^{-6} SI for the lower part (10.12–18.4 m). The lower part from Nu 18.0–12.0 shows values from 0.052–0.028 (mean 0.039). Above Nu 12.0 values range from 0.050–0.026 (mean 0.033). The most marked change appears at Nu 10.0 from values of 0.050 to 0.010. The upper interval from Nu 10.0 to 0.0 is characterized by very low values from 0.012–0.000 (mean 0.004). The J/K boundary strata itself are not characterized by significant changes in values.

Gamma log

The radioactivity variation of the studied section is measured by gamma-ray measures and represents a direct function of the variation of the clay-mineral content. Hence, higher radioactivity reflects higher clay contents. Measurements of gamma response (cps) are a powerful tool for interpreting the stratigraphy in the outcrop.

Generally measured cps values range between 4 and 30. The gamma response allows a clear subdivision of the section into three parts each corresponding to the three identified main lithological units within the Blassenstein Formation. The gamma response gradually decreases from Nu 18.0 to Nu 0.0, reaching the highest values at Nu 16.5 and lowest values at Nu 7.7 and Nu 3.3. Within this gradually decreasing trend, the biggest excursion is recorded close to bed Nu 10.0. Values range in the lower interval (Nu 18.0–12.0) from 15–30 cps (mean 22.53 cps), in the middle interval (Nu 12.0–10.0) from 13–23 cps (mean 19.95 cps), and in the upper interval (Nu 10.0–0.0) from 4–14 cps (mean 9.07 cps) (Fig. 3).

The gamma response becomes gradually weaker in the upper, undisturbed part of the section. The uppermost part of the section, however, shows an upwards decreasing gamma response. The curve pattern therefore shows a vertically congruent curve to the susceptibility values.

The decreasing gamma log values together with the characteristic pattern in decreasing susceptibility suggest a more stable depositional environment from about Nu 10.0 and upwards, predating the J/K boundary by 3 meters or 0.5 million years.

Paleomagnetism

The paleomagnetic study of the section identifies the boundaries of magnetozones from M17r to M21r and the reverse subzones Kysuca and Brodno (M20n.1r and M19n.1r, respectively). The record of polarity changes in the Earth's magnetic field can determine the precise age. The identification of the detected polarity zones against the M-sequence of polarity intervals given by the GPTS (Gradstein et al. 2004) is the most important topic. The preliminary determination of boundaries of magnetozones M17n to M22r was the result from 30 samples of C-component direction (Pruner et al. 2009). The number of polarity zones, namely six normal and six reverse, is the same number as in preliminary results. The mean values of the modulus of NRM (Jn) and of volume magnetic susceptibility (k) for 244 samples of Upper Tithonian and Lower Berriasian limestones are shown in Table 1. The k ranges from –8.6 to 15.6×10^{-6} SI for the upper interval between 0–10 m of the section and from 30 to 85.1×10^{-6} SI for the lower part (10.12–18.4 m). The results of AF and TD demagnetization procedures are displayed in Pruner et al. (2009: figs. 3, 4). The A-component is of viscous origin and is demagnetizable in the temperature range of 20–100 °C (or AF 0–5 mT). The origin of the B-components, low temperature (LTC) or low field (LFC) were undoubtedly imprinted, most probably in the Neogene, after Alpine folding. Both magnetic polarities are present in C-component (high temperature — HTC or high field — HFC) directions, but the directions are highly scattered (Table 2, Fig. 5). The statistical

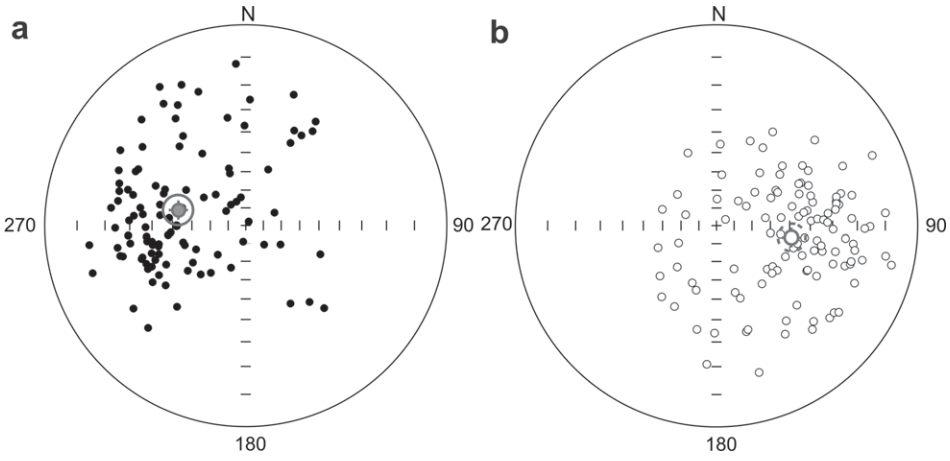

Fig. 5. J/K limestones and marls, directions of N polarity (left) and R polarity (right) of C-components of RM corrected for dip of strata. Stereographic projection, full (open) small circles represent projection onto the lower (upper) hemisphere. The mean direction calculated according to Fisher (1953) is marked by a small crossed circle, the confidence circle at the 95% probability level is circumscribed about the mean direction.

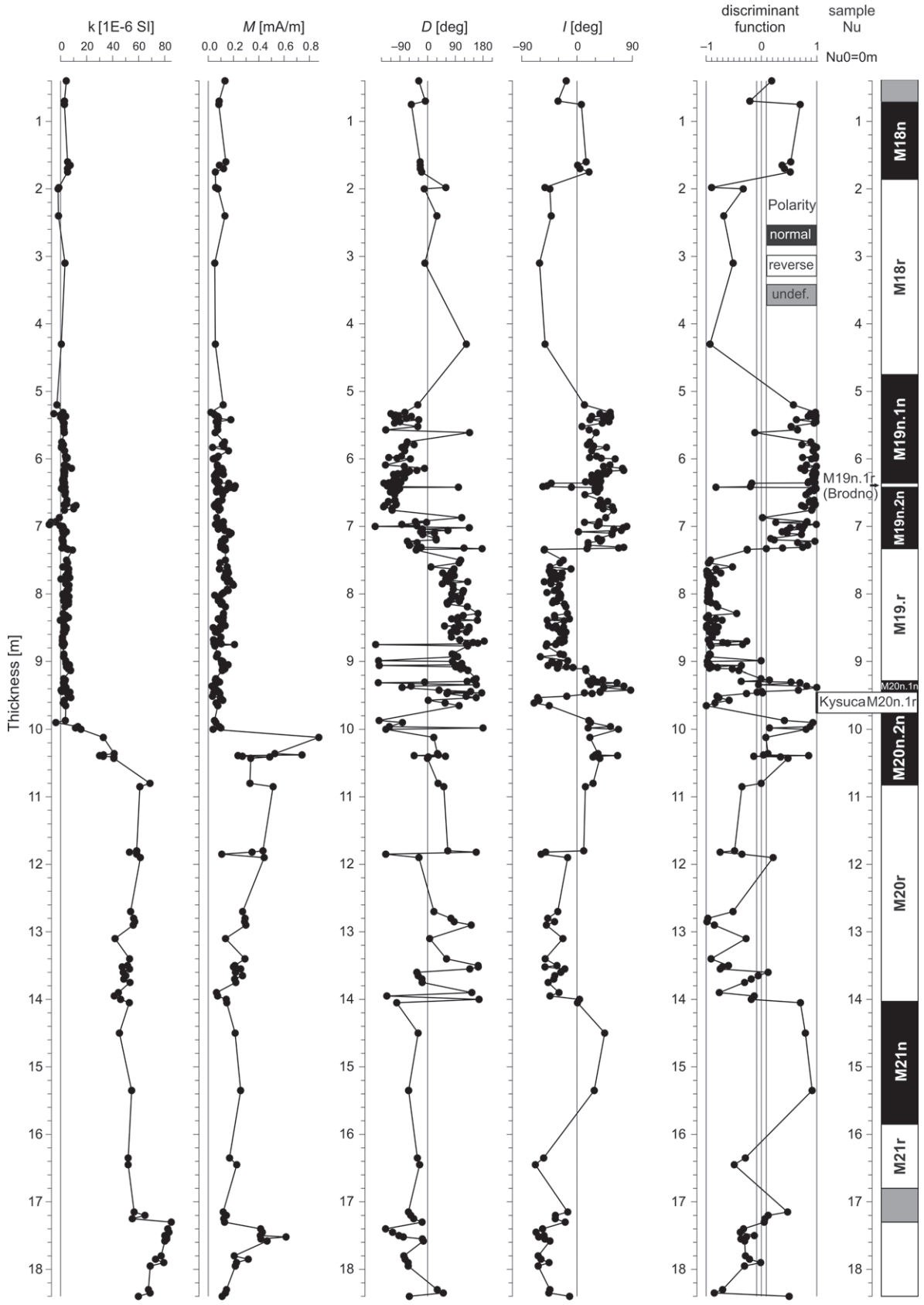

Fig. 6. Magnetostratigraphic profile across the Nutzhof J/K boundary strata, paleomagnetic and lithostratigraphic data. *M* — NRM in the natural state; *k* — value of volume magnetic susceptibility in the natural state; D — declination; I — inclination. Normal (reverse) magnetozones are denoted black (white), unknown (grey).

Table 1: Basic magnetic parameters and statistical properties of the physical quantities in the basic groups of samples from the Nutzhof.

Age	Polarity	Number of samples	Modulus of NRM J_n [10^{-6} A/m]		Volume magnetic susceptibility k [10^{-6} SI]	
			Mean value	Standard deviation	Mean value	Standard deviation
Early Berriasian	N+R	82	88	39	2.3	3.1
Late Tithonian	N+R	155	165	132	21.4	26.5

Table 2: Mean directions of B (LFC or LTD) and C-components (HFC or HTD) corrected and not corrected for structural tilt.

Age of rocks	Component of remanence	Polarity	Structural tilt correction				No structural tilt correction (in-situ directions)				n
			Mean directions		α_{95} [°]	k	Mean directions		α_{95} [°]	k	
			Decl. [°]	Incl. [°]			Decl. [°]	Incl. [°]			
L. Tith.+ E.Berr.	B	R	351.7	–55.4	3.1	12.1	10.4	77.5	3.1	11.9	168
L. Tith.+ E.Berr.	C	N	278.0	53.3	7.1	3.2	199.3	–27.3	8.0	2.6	119
L. Tith.+ E.Berr.	C	R	104.1	–46.1	6.4	4.8	19.3	13.2	6.4	4.8	101
L. Tith.+ E.Berr.	C	N*)	286.1	44.5	4.7	4.0	198.1	–15.0	5.2	3.7	220

parameters for component C (total number 220) are influenced by samples close to the boundary of shorter polarity zones. The mean values of C-component directions are anomalous, having been affected by counter clockwise paleotectonic rotation. The paleomagnetic data given in the magnetostratigraphic profile (Fig. 6) indicate a significant change of remanent magnetization and magnetic susceptibility, at level Nu 10 due to the significant change in lithology from marl (Nu 18.0–10.0) to limestone (Nu 10.0–0.0).

Figure 5 presents the results of the magnetostratigraphic profile with indicated moduli values of natural remanent magnetization (*Jn*), volume magnetic susceptibility values of samples in the natural state (*k*), paleomagnetic declination Dp and inclination Ip (of C-components of remanence inferred by multi-component analysis). The values of the angular deflection of the direction of C-components of remanence from the mean direction, with only normal polarity being taken into consideration (reverse directions were transformed into normal directions for the calculation of the mean direction), are given in the next column. The resulting normal and reverse magnetozones are indicated in the last column.

Discussion

The high-resolution quantitative analysis of selected organic groups (calpionellids, radiolarians, saccocomids) indicates major variations in their abundance and composition (Figs. 2, 3, 4). The Upper Jurassic (Tithonian) depositional setting at Nutzhof was influenced by the periodic input of biodetritus from surrounding shallow marine paleoenvironments, whereas deposition was more constant during the Berriasian and characterized by pelagic sediments predominantly composed of planktonic microorganisms (radiolarians, calcareous dinoflagellates, calpionellids, and nannofossils).

Calcareous dinoflagellates predominate in the Lower and Upper Tithonian. Their stratigraphic and paleoecological potential has been discussed by Reháková (2000a,b). In the Nutzhof section, the Lower Tithonian record of calcareous dinoflagellates shows a distinct change in abundance and composition. Forms with radial orientation of calcite crystallites in their cyst walls dominate in the *Tithonica* and *Malmica* Zones, whereas cadosinid species with oblique arrangement of the calcite crystallites dominate the *Semiradiata* Zone. According to Michalík et al. (2009), coinciding acme peaks of *Cadosina semiradiata semiradiata* Wanner and *Conusphaera* spp. probably indicate warmer surface waters.

Chitinoidellids are very rare in the Nutzhof section. The appearance of the first hyaline calpionellid loricas precedes the crassicollarian radiation. A monospecific calpionellid association consisting predominantly of *Calpionella alpina* Lorenz characterizes the section. A similar calpionellid evolution and biostratigraphy of the Jurassic-Cretaceous boundary interval was recorded by Remane (1986), Pop (1994), Reháková (1995), Olóriz et al. (1995), Grün & Blau (1997), and Andreini et al. (2007). Reháková (in Michalík et al. 2009) demonstrated that the J/K boundary interval can be characterized by several calpionellid events: the onset, diversification, and extinction of chitinoidellids (middle Tithonian); the onset, diversification, and extinction of crassicollarians (Upper Tithonian); and the onset of the monospecific *Calpionella alpina* association at the J/K boundary. Due to synsedimentary erosion probably originating during several extensional pulses, which denivelated the sea bottom, clast-bearing calpionellid biomicrites were documented along the Upper Jurassic and Lower Cretaceous (Lower Berriasian) formations in several areas studied (Michalík et al. 1990, 1995; Grabowski et al. 2010).

The calcareous nannofossil ranges in the Nutzhof section provides a tool for biostratigraphic subdivision of the J/K boundary interval. The coccoliths of the family Watznaueriaceae and three nannolithic genera *Conusphaera*, *Polycostella*, and *Nannoconus* dominate the assemblages. This is in accordance with nannofossil studies in other locations at low latitudes sections across the J/K boundary (Thierstein 1971, 1973, 1975; Erba 1989; Gardin & Manivit 1993; Özkan 1993;

Tavera et al. 1994; Bornemann et al. 2003; Pszczółkowski & Myczyński 2004; Tremolada et al. 2006; Halásová in Michalík et al. 2009).

The lowermost occurrences of nannofossils are partly obscured due to poor preservation, but we tentatively identified the boundaries of zones and subzones based on certain stratigraphic markers (*Polycostella beckmannii*, *Helenea chiastia*, *Hexalithus noeliae*, *Nannoconus wintereri*, *Nannoconus globulus minor*, *Nannoconus steinmannii minor*, *Nannoconus kamptneri minor*, *Nannoconus steinmannii steinmannii*, *Nannoconus kamptneri kamptneri*, *Nannoconus globulus globulus*).

Tremolada et al. (2006) detected that *Conusphaera* dominates the nannolith assemblage in the upper middle Tithonian ("*Conusphaera* world"). This is corroborated by data obtained in this study. The acme peak of the genus *Polycostella* in samples Nu 13.0 and 14.0 coincides with the middle Tithonian *Semiradiata* Subzone (Reháková 2000b). Comparison with the Brodno section (Michalík et al. 2007 and Michalík et al. 2009) indicate that the dominance of the nannolith *Polycostella beckmannii* occurs somewhat lower in the *Chitinoidella* Zone in the Nutzhof section. The first appearance of *Helenea chiastia* is also demonstrated to be diachronous, being close to the base of the calpionellid *Crassicollaria* Zone in the Brodno section, but recorded in the uppermost part of the *Chitinoidella* Zone in the Nutzhof section.

The most distinct nannofossil event is the onset of nannoconids which was observed in the interval comprising the calpionellid *Calpionella* Zone, *Ferasini* Subzone (lowermost Berriasian). This indicates a change in the paleooceanographic regime. From the biostratigraphic point of view, the upper J/K boundary datum based on nannofossils (Bornemann et al. 2003).

The change of saccocomid marl and limestone by overlying calpionellid limestone in the Upper Tithonian also characterizes J/K-boundary successions reported from numerous other localities in Austria (e.g. Kristan-Tollmann 1962; Flügel 1967; Holzer 1968; Holzer & Poltnik 1980; Reháková et al. 1996), Germany (Lackschewitz et al. 1989), Poland (Pszczółkowski & Myczyński 2004) and Slovakia (Vašíček et al. 1992). Many of these localities, however, differ lithologically from the section studied at Nutzhof. In most cases the saccocomid-bearing beds are pure, reddish limestone.

Saccocomid limestones have often been interpreted as Kimmeridgian (e.g. Flügel 1967: p. 35; Sauer et al. 1992: p. 183; Wessely 2008: p. 210, fig. 5) and have been used as the marker bed for that stage (Bernouli 1972). Reliable stratigraphic data is, however, commonly lacking. Based on well-dated sections, the majority of the recorded saccocomid-occurrences are of Tithonian age (Nicosia & Parisi 1979; Keupp & Matyszkiewicz 1997). This is corroborated/supported by the data from the present study.

Summary and conclusions

The studied section at Nutzhof represent a J/K-boundary succession deposited in a distal slope-setting in the Gresten Klippenbelt, a part of the Helvetic paleogeographic realm. The Upper Jurassic to Lower Cretaceous pelagic sediments represent a major sedimentation cycle.

The significant depositional change from a mixed siliciclastic/carbonate to a pure carbonate depositional system is marked by a change from a lower marly cyclic part to an upper calcareous part. Accordingly, the lower (Tithonian) marly part is characterized by dark, laminated pelagic marls and marly limestones with intercalated turbiditic limestone beds (e.g. allodapic limestones). The upper part (limestone) represents a phase of autochthonous pelagic sedimentation characterized by bright, chert- and aptychi-bearing nannoconid limestone. The macro-invertebrate fauna of the Berriasian limestone succession is sparse, comprising rare ammonoids, aptychi, belemnites and brachiopods. The macro-invertebrate fauna of the Tithonian marl-limestone succession is rich in saccocomids accompanied by rare bivalves (inoceramids) and partly by abundant ammonites. The microfauna, in contrast, is abundant, with dominating calpionellids and radiolarians in the limestone succession and saccocomid blooms within the marl-limestone succession.

The macrofauna, as already stated, is represented especially by ammonoids, belemnoids, aptychi and bivalves. The whole section yielded 46 ammonite individuals/specimens. Sampling of the sparse ammonites was difficult due to hardite sediments. The ammonite biostratigraphy is integrated with micro- and nannofossil biostratigraphic data from the marl-limestone succession and indicates Early Tithonian to middle Berriasian ages (*Hybonoticeras hybonotum* Zone up to the *Subthurmannia occitanica* Zone). Descendants of *Subplanites* have not previously been reported within the Gresten Klippenbelt. All ammonoids are typical of the Mediterranean Province.

The limitation of ammonite biostratigraphy obtained by the new ammonite findings from Nutzhof has demonstrated the importance of integrating macrofauna biostratigraphy with the micro- and nannofossil biostratigraphy. The described fauna increases our understanding of ammonite faunas from the area of the Gresten Klippenbelt and the neighbouring Waschberg Zone during deposition of the Jurassic/Cretaceous boundary interval. Both areas were at the time located on the passive northern margin of the Penninic Ocean.

Magnetostratigraphic, geochemical and isotopes studies contribute to the understanding of the environmental history during the Jurassic-Cretaceous boundary interval in a little known area. Sediment deposition took place during conditions of relatively stable water masses with relatively low sedimentation rates in an unstable sedimentological environment. This is reflected by a change in lithology from Nu 11.0 to Nu 13.0 (11 to 13 m). A series of event layers with redeposited faunal elements (e.g. phyllocrinids) indicate a transport of sediment from shallower areas in the North. The depositional area was influenced by the opening of the Penninic Ocean during the Late Jurassic to Early Cretaceous. A phase of an earlier Penninic opening, is reflected as a significant change in lithology and composition of faunal assemblage in the uppermost Tithonian (at Nu 10.0 m).

There is no evidence for redeposition of ammonites, which are considered autochthonous and parautochthonous pelagic elements from the open sea. Four crinoid taxa are recorded in

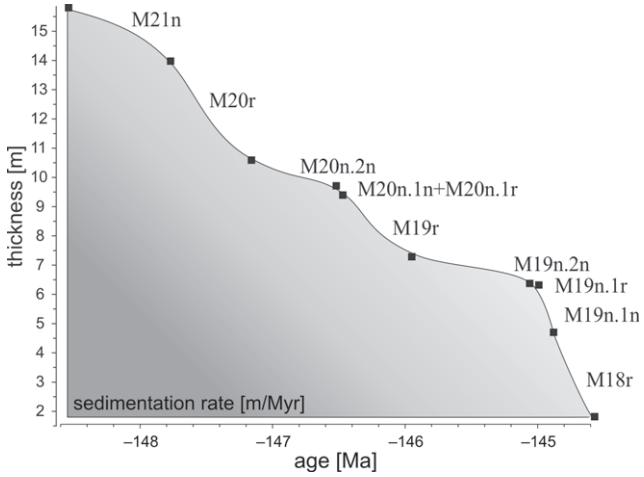

Fig. 7. Estimated average sedimentation rate diagram around the J/K boundary at Nutzhof based on magnetostratigraphic and biostratigraphic data.

the Tithonian Blassenstein Formation and comprise *Balanocrinus* sp., *Saccocoma tenella* (Goldfuss), *Crassicoma*? sp., and *Phyllocrinus belbekensis* Arendt. Only *S. tenella* is abundant. The other taxa, in particular the benthic isocrinids and phyllocrinids are rare. Preservation and ossicle size range of the latter groups indicate their allochthonous origin. The saccocomid remains are restricted to the Tithonian, the saccocomid-rich facies being overlain by calpionellid limestones.

The biostratigraphic study based on the distribution of calpionellids allowed an identification of the *Boneti* Subzone of the *Chitinoidella* Zone. The J/K boundary is recorded between the *Crassicollaria* and *Calpionella* Zone and is defined by the morphological change of *Calpionella alpina* tests. The base of the *Crassicollaria* Zone approximately coincides with the onset of *Tintinnopsella remanei* Borza and the base of the standard *Calpionella* Zone, with the monospecific calpionellid association being dominated by *Calpionella alpina* Lorenz. Two further Subzones (*Ferasini* and *Elliptica*) of the standard *Calpionella* Zone were recognized in radiolarian-calpionellid and calpionellid-radiolarian wackestones in the overlying uppermost part of the section.

The appearance of several important nannofossil genera allow the identification of the Lower, middle and Upper Tithonian, and a relatively accurate identification of the Tithonian-Berriasian boundary, and the definition of the Lower Berriasian nannofossil zones. Coccoliths of the family Watznaueriaceae and nannoliths of the genera *Conusphaera*, *Nannoconus* and *Polycostella* dominate the assemblages. The interval between the FAD of *Nannoconus wintereri* co-occurring with small nannoconids in sample Nu 9 (the uppermost Tithonian) and the FAD of *Nannoconus kamptneri minor* in sample Nu 5 (lowermost Berriasian) is interpreted as the Tithonian-Berriasian boundary interval. The nannoconid dominance in the lowermost Berriasian, known as the "*Nannoconus* world" sensu Tremolada et al. (2006) is now recorded in the Nutzhof section.

Paleomagnetic data across the J/K boundary strata allow the construction of a detailed magnetostratigraphic zonation. The interval between Nu 5 to 10.5 m provides a high-resolution profile with an almost continuous record of magnetic and paleomagnetic parameters, that records the critical intervals with boundaries of the magnetozones M19n–M20n. According to magnetozone M19n and Brodno Subzone, the J/K boundary is identified within the interval between Nu 6.5–7 m. Significant changes do not occur at the J/K boundary itself. The step of remanent magnetization and magnetic susceptibility, at level Nu 10.0, occurs in magnetozone M20n below the Kysuca Subzone. A similar jump of NRM and susceptibility lies in the M20n just above the Kysuca Subzone in the Bosso section. The average sedimentation rate in the Nutzhof section is ca. 3.7 m/Myr (Fig. 7), but with high dispersion (from 2–11 m/Myr) differing from the average sedimentation rates of 2.27 m/Myr recorded in Brodno and 2.88 m/Myr in Puerto Escaño. Relatively low rates (1 m/Myr) are recorded in the Bosso Valley, but higher rates (3–11 m/Myr) are reported by Grabowski & Pszczółkowski (2006) from the Tatra Mountains. No significant change can be noted at or within the J/K boundary interval. The integration of fossil and magnetostratigraphic data demonstrates a duration of approximately 7 million years (approximately 150–143 Ma) for the deposition of the Nutzhof section (Figs. 6 and 7).

The carbon isotope record documents a significant change in the C-cycle dynamic suggesting a sluggish 3-D dynamic of the marine system possibly associated with a decrease in primary productivity. Abrupt oscillations mainly recorded between the levels 10 and 6 m suggest a significantly unstable global carbon system during the Jurassic but a change towards balanced conditions in the Cretaceous interval.

Acknowledgments: We are indebted to Hans Egger (Geological Survey of Austria) who made us aware of the studied locality. The study was supported by the Austrian Science Fund (FWF; Project P20018-N10) and by the Grant Agency of the Czech Republic (Grant No. GACR 205-07-1365) and Research Plan of the IG AS CR No. CEZ AV0Z30130516. This is also a contribution to the 506 IGCP UNESCO Project, APVV-0280-07, APVV-0248-07, APVV- 0465-06, APVT 51-011305 and LPP 0120-09. MW thanks IGCP 555 and the Austrian Academy of Sciences for financial support. Thanks go to members of the Kilian Group (Lower Cretaceous Ammonite Working Group; president Stephane Reboulet, Lyon) for fruitful discussions on the ammonoid fauna. Technical support for photography was provided by Alice Schumacher (Vienna). Franz Topka (Vienna) assisted with the preparation of ammonoid specimens and Anton Englert (Vienna) prepared the thin sections. Paleomagnetic analyses were performed by Daniela Venhodová, Jana Drahotová, and Jiří Petráček. The software for the evaluation of paleomagnetic measurements was prepared by Otakar Man (Institute of Geology ASCR v.v.i.). We thank Luc Bulot (Marseille) and Jacek Grabowski (Warsaw) for their comments which helped to improve the quality of the manuscript.

References

Andreini G., Caracuel J.E. & Parisi G. 2007: Calpionellid biostratigraphy of the Upper Tithonian–Upper Valanginian inter-

val in Western Sicily (Italy). *Swiss J. Geosci*. 100, 179–198.
Bernouli D. 1972: North Atlantic and Mediterranean Mesozoic facies: A comparison. *Init. Repts. DSDP* 11, 631–643.
Bornemann A., Aschwer U. & Mutterlose J. 2003: The impact of calcareous nannofossils on the pelagic carbonate accumulation across the Jurassic-Cretaceous boundary interval. *Palaeogeogr. Palaeoclimatol. Palaeoecol*. 199, 187–228.
Bralower T.J., Monechi S. & Thierstein H.R. 1989: Calcareous nannofossil zonation of the Jurassic-Cretaceous boundary interval and correlation with the geomagnetic polarity timescale. *Mar. Micropaleont*. 14, 153–235.
Čžjžek J. 1852: Aptychenschiefer in Niederösterreich. *Jb. K.-Kön. Geol. Reichsanst.* 3, 3, 1–7.
Decker K. 1990: Plate tectonics and pelagic facies: Late Jurassic to Early Cretaceous deep-sea sediments of the Ybbsitz ophiolite unit (Estern Alps, Austria). *Sed. Geol*. 67, 85–99.
Decker K. & Rögl F. 1990: Early Cretaceous agglutinated foraminifera from limestone-marly rhythmites of the Gresten Klippen Belt (Eastern Alps Austria). *Abh. Geol. B.–A*. 41, 41–59.
Dercourt J., Ricou L.E. & Vrielynck B. (Eds.) 1993: Atlas Tethys palaeoenvironment maps, 14 maps, 1 pl. *Gauthier-Villars*, Paris, 1–307.
Dercourt J., Gaetani M., Vrielynck B., Barrier E., Biju Duval B., Brunet M.F., Cadet J.P., Crasquin S. & Sandulescu M. (Eds.) 2000: Atlas Peri-Tethys, Palaeogeographical maps, 24 maps and explanatory notes: I-XX. *CCGM/CGMW*, Paris, 1–269.
Erba E. 1989: Calcareous nannofossil zonation of the Jurassic-Cretaceous boundary interval and correlation with the geomagnetic polarity timescale. *Mar. Micropaleont*. 14, 153–235.
Faupl P. 2003: Historische Geologie: eine Einführung. *Facultas*, Wien, 1–271.
Faupl P. & Wagreich M. 2000: Late Jurassic to Eocene Palaeogeography and Geodynamic Evolution of the Eastern Alps. *Mitt. Österr. Geol. Gesell*. 92, 79–94.
Fisher R.A. 1953: Dispersion on a sphere. *Proc. R. Soc. London A*. 217, 295–305.
Flügel H.W. 1967: Die Lithogenese der Steinmühl-Kalke des Arracher Steinbruches (Jura, Österreich). *Sedimentology* 9, 23–53.
Gardin S. & Manivit H. 1993: Upper Tithonian and Berriasian calcareous nannofossils from the Vocontian Trough (SE France): Biostratigraphy and sequence stratigraphy. *Bull. Centres Rech. Explor.-Prod. Elf-Aquitaine* 17, 1, 277–289.
Gottschling P. 1965: Zur Geologie der Hauptklippenzone und der Laaber Teildecke im Bereich von Glashütte bis Bernreith (Niederösterreich). *Mitt. Geol. Gesell. Wien* 58, 23–86.
Grabowski J. & Pszczółkowski A. 2006: Magneto- and biostratigraphy of the Tithonian-Berriasian pelagic sediments in the Tatra Mountains (central Western Carpathians, Poland): sedimentary and rock magnetic changes at the Jurassic/Cretaceous boundary. *Cret. Research* 27, 398–417.
Grabowski J., Michalík J., Pszczółkowski A. & Lintnerová O. 2010: Magneto-, and isotope stratigraphy around the Jurassic/Cretaceous boundary in the Vysoká Unit (Malé Karpaty Mts, Slovakia): correlations and tectonic implications. *Geol. Carpathica* 61, 4, 309–326.
Gradstein F.M., Ogg J.G. & Smith A.G. (Eds.) 2004: A geologic time scale 2004. *Cambridge University Press*, Cambridge, U.K., 1–589.
Grün B. & Blau J. 1997: New aspects of calpionellid biochronology: proposal for a revised calpionellid zonal and subzonal division. *Rev. Paléobiol.* 16, 197–214.
Hardenbol J., Thierry J., Farley M.B., Jacquin T., de Graciansky P.C. & Vail P.R. 1998: Mesozoic and Cenozoic sequence stratigraphy of European basins. *SEPM, Spec. Publ*., Tulsa 60, 1998.
Hennig S., Weissert H. & Bulot L. 1999: C-isotope stratigraphy, a calibration tool between ammonite- and magnetostratigraphy: the Valanginian-Hauterivian transition. *Geol. Carpathica* 50, 91–96.
Hess H., Ausich W.I., Brett C.E. & Simms M.J. 1999: Fossil crinoids. *Cambridge University Press*, Cambridge, MA, xv+275.
Hirano H. 1993: Phyletic evolution of desmoceratine ammonoids through the Cenomanian-Turonian oceanic anoxic event. In: House M.R. (Ed.): The Ammonoidea: environment, ecology, and evolutionary change. *Clarendon Press*, Oxford, UK, 267–283.
Holzer H.-L. 1968: Stratigraphie und Lithologie der Jura-Kreide-Folge im nördlichsten Pechgraben-Steinbruch. *Mitt. Naturwiss. Vereins Steiermark* 98, 47–57.
Holzer H.-L. & Poltnig W. 1980: Erster Nachweis einer Radialplatten-Fossillagerstätte der Schwebcrinoide *Saccocoma* im oberostalpinen Malm (Ostkarawanken, Kärnten). *Carinthia II* 170, 201–216.
Houša V., Krs M., Krsová M., Man O., Pruner P. & Venhodová D. 1999: High-resolution magnetostratigraphy and micropaleontology across the J/K boundary strata at Brodno near Žilina, western Slovakia: summary results. *Cret. Research* 20, 699–717.
Houša V., Krs M., Man O., Pruner P., Venhodová D., Cecca F., Nardi G. & Piscitello M. 2004: Combined magnetostratigraphic, paleomagnetic and calpionellid investigations across Jurassic/Cretaceous boundary strata in the Bosso Valley, Umbria, central Italy. *Cret. Research* 25, 771–785.
Keupp H. & Matyszkiewicz J. 1997: Zur Faziesrelevanz von *Saccocoma*-Resten (Schwebcrinoiden) in Oberjura-Kalken des nördlichen Tethys-Schelfs. *Geol. Blätter für Nordost-Bayern und angrenzende Gebiete* 47, 53–70.
Kirschvink J.L. 1980: The least-squares line and plane and the analysis of palaeomagnetic data. *Geophys. J. Roy. Astr. Soc*. 62, 699–718.
Kristan-Tollmann E. 1962: Stratigraphisch wertvolle Mikrofossilien aus dem Oberjura und Neokom der Nördlichen Kalkalpen. *Erdoel-Z*. 78, 637–549.
Kroh A. & Lukeneder A. 2009: Crinoids from the Late Jurassic–Early Cretaceous of the Nutzhof section (Lower Austria, Pieniny Klippenbelt). *Ann. Naturhist. Mus. Wien*, *Serie A* 110, 383–399.
Kühn O. 1962: Autriche. *Lexique Stratigr. Int.*, Europe 8, 1–646.
Küpper H. 1962: Beobachtungen in der Hauptklippenzone bei Stollberg, N.Ö. *Verh. Geol. B.–A*. 2, 263–268.
Lackschewitz K., Grützmacher U., Suhr J. & Kiel R.H. 1989: Synsedimentäre Kippschollentektonik: Becken- und Schwellenfazies oberjurassischer Karbonate der Chiemgauer Alpen. *Geol. Paläont. Mitt. Innsbruck* 16, 163–165.
Lierl H.J. 1992: Tenside — ihre Verwendung für die Präperation geologisch-paläontologischer Objekte. *Der Präperator* 38, 12–17.
Lukeneder A. 2009: New biostratigraphic ammonite data from the Jurassic/Cretaceous boundary at Nutzhof (Gresten Klippenbelt, Lower Austria). *Ann. Naturhist. Mus. Wien*, *Serie A* 110, 313–330.
Mandic O. & Lukeneder A. 2008: Dating the Penninic Ocean subduction: new data from planktonic foraminifera. *Cret. Research* 29, 901–912.
Masse J.P. et al. (12 co-authors) 2000: Early Aptian. In: Dercourt J., Gaetani M. et al. (Eds.). Atlas Peri-Tethys, Palaeogeographical Maps 13, (CCGM/CGMW) Paris.
McArthur J.M. & Howarth R.J. 2004: Strontium isotope stratigraphy. In: Gradstein F.M., Agterberg F.P. & Smith A.G. (Eds.): A geologic time scale 2004. *Cambridge University Press*, 96–105.
McArthur J.M., Howarth R.J. & Bailey T.R. 2001: Strontium isotope stratigraphy: LOWESS Version 3: best fit to the marine Sr-isotope curve for 0–509 Ma and accompanying look-up table for deriving numerical age. *J. Geol*. 109, 155–170.
McArthur J.M., Janssen N.M.M., Reboulet S., Leng M.J., Thirlwall

M.F. & van de Schootbrugge B. 2007: Early Cretaceous ice-cap volume, palaeo-temperatures (Mg, ^{18}O), and isotope stratigraphy (^{13}C, $^{87}Sr/^{86}Sr$) from Tethyan belemnites. *Palaeogeogr. Palaeoclimatol. Palaeoecol.* 248, 391–430.

Michalík J., Reháková D. & Halásová E. 1990: Stratigraphy of the Jurassic/Cretaceous boundary beds in the Hlboč Valley (Vysoká Unit of the Krížna Nappe, Malé Karpaty Mts). *Knihovnička ZPN* 9a, 183–204 (in Slovak, with English summary).

Michalík J., Reháková D. & Vašíček Z. 1995: Early Cretaceous sedimentary changes in west Carpathian area. *Geol. Carpathica* 46, 285–296.

Michalík J., Reháková D., Halásová E. & Lintnerová O. 2007: Integrated stratigraphy of the Jurassic/Cretaceous boundary at the Brodno section (the Kysuca Unit, Pieniny Klippen Belt, Western Carpathians). *Abstract book, International geological correlation programme 506 — Jurassic marine: non-marine correlation*, *Univ. Bristol*, 1–3.

Michalík J., Reháková D., Halásová E. & Lintnerová O. 2009: A possible West Carpathian regional stratotype of the Jurassic/Cretaceous boundary (the Brodno section near Žilina). *Geol. Carpathica* 60, 3, 213–232.

Nicosia U. & Parisi G. 1979: *Saccocoma tenella* (Goldfuss) — Distribuzione stratigrafica e geografica. *Boll. Soc. Paleont. Ital.* 18, 320–326.

Olóriz F., Caracuel J.E., Marques B. & Rodríguez-Tovar F.J. 1995: Asociaciones de Tintinnoides en facies Ammonitico Rosso de la Sierra Norte (Mallorca). *Rev. Esp. Paleont., No. Homenaje al Dr. G. Colom*, 77–93.

Özkan S. 1993: Calcareous nannofossils from the Late Jurassic–Early Cretaceous of Northwest Anatolia, Turkey. *Geol. J.* 28/3–4, 295–307.

Piller W. et al. 2004: Die Stratigraphische Tabelle von Österreich 2004 (sedimentäre Schichtfolgen). *Österr. Akad. Wissenschaft. Österr. Stratigr. Kommission*, Wien.

Pop G. 1994: Calpionellid evolutive events and their use in biostratigraphy. *Rom. J. Stratigraphy* 76, 7–24.

Pop G. 1997: Révision systématique des chitinoidelles tithoniennes des carpathes méridionales (Roumanie). *Compt. Rendus Acad. des Sci., Sér. IIa*, Paris 342, 931–938.

Pruner P., Schnabl P. & Lukeneder A. 2009: Preliminary results of magnetostratigraphic investigations across the Jurassic/Cretaceous boundary strata in the Nutzhof, Austria. *Ann. Naturhist. Mus. Wien*, *Ser. A* 110, 331–344.

Pszczółkowski A. & Myczyński R. 2004: Ammonite-supported microfossil and nannoconid stratigraphy of the Tithonian-Hauterivian limestones in selected sections of the Branisko Succession, Pieniny Klippen Belt (Poland). *Stud. Geol. Pol.* 123, 133–197.

Reháková D. 1995: New data on calpionellid distribution in the Upper Jurassic/Lower Cretaceous formations (Western Carpathians). *Miner. Slovaca* 27, 308–318 (in Slovak).

Reháková D. 1998: Calpionellid genus *Remaniella* Catalano 1956 in Lower Cretaceous pelagic deposits of Western Carpathians. *Miner. Slovaca* 30, 443–452.

Reháková D. 2000a: Calcareous dinoflagellate and calpinellid bioevents versus sea-level fluctuations recorded in the West-Carpathian (Late Jurassic/Early Cretaceous) pelagic environments. *Geol. Carpathica* 51, 4, 229–243.

Reháková D. 2000b: Evolution and distribution of the Late Jurassic and Early Cretaceous calcareous dinoflagellates recorded in the Western Carpathian pelagic carbonate facies. *Miner. Slovaca* 32, 79–88.

Reháková D. 2002: *Chitinoidella* Trejo, 1975 in Middle Tithonian carbonate pelagic sequences of the West Carpathian Tethyan area. *Geol. Carpathica* 55, 6, 369–379.

Reháková D. & Michalík J. 1997: Evolution and distribution of calpionellids — the most characteristic constituents of Lower Cretaceous Tethyan microplankton. *Cret. Research* 18, 493–504.

Reháková D., Michalík J. & Ožvoldová L. 1996: New microbiostratigraphical data from several Lower Cretaceous pelagic sequences of the Northern Calcareous Alps, Austria (Preliminary results). *Geol. Paläont. Mitt. Innsbruck* 4, 57–81.

Reháková D., Halásová E. & Lukeneder A. 2008: The Jurassic/Cretaceous boundary in the Austrian Klippen belt (Nutzhof, Lower Austria): Implications on micro- and nannofacies analysis. *Ber. Geol. B.–A.* 74, 95–97.

Reháková D., Halásová E. & Lukeneder A. 2009: The Jurassic-Cretaceous boundary in the Austrian Klippen Belt (Nutzhof, Lower Austria): Implications on Micro- and Nannofacies analysis. *Ann. Naturhist. Mus. Wien*, *Ser. A* 110, 345–381.

Remane J. 1986: Calpionellids and the Jurassic-Cretaceous boundary. *Acta Geol. Hung.* 29, 15–26.

Roth P.H., Medd A.W. & Watkins D.K. 1983: Jurassic calcareous nannofossil zonation, an overview with new evidence from Deep Sea Drilling Project Site 534A. In: Sheridan R.E., Gradstein F.M. et al. *Init. Repts. DSDP* 76, 573–579.

Řehánek J. 1992: Valuable species of cadosinids and stomiosphaerids for determination of the Jurassic-Cretaceous boundary (vertical distribution, biozonation). *Scripta* 22, 117–122.

Sauer R., Seifert P. & Wessely G. 1992: Guidebook to excursions in the Vienna Basin and the adjacent Alpine-Carpathian Thrustbelt in Austria. Part II. *Mitt. Österr. Geol. Gesell.* 85, 97–239.

Scotese C.R. 2001: Atlas of earth history. *Paleomap project*, Arlington, Texas, 1–52.

Spötl C. & Vennemann T. 2003: Continuous-flow isotope ratio mass spectrometric analysis of carbonate minerals. *Rapid Communications in Mass Spectrometry* 17, 1004–1006.

Stampfli G.M. & Borel G.D. 2002: A plate tectonic model for the Paleozoic and Mesozoic constrained by dynamic plate boundaries and restored synthetic oceanic isochrons. *Earth Planet. Sci. Lett.* 196, 17–33.

Stampfli G. & Mosar J. 1999: The making and becoming of Apulia. *Mem. Sci. Géol. Padova. Spec. Vol.*, *3rd Workshop on Alpine Geology* 51/1, 141–154.

Stampfli G.M., Borel G.D., Marchant R. & Mosar J. 2002: Western Alps geological constraints on western Tethyan reconstructions. In: Rosenbaum G. & Lister G.S. (Eds.): Reconstruction of the evolution of the Alpine-Himalayan Orogen. *J. Virtual Explorer* 8, 77–106.

Tavera J.M., Aguado R., Company M. & Olóriz F. 1994: Integrated biostratigraphy of the Durangites and Jacobi Zones (J/K boundary) at the Puerto Escaño section in Southern Spain (province of Cordoba). *Geobios* 17, 469–476.

Thierstein H. 1971: Tentantive Lower Cretaceous calcareous Nanoplankton Zonation. *Eclogae Geol. Helv.* 64, 3, 437–652.

Thierstein H. 1973: Lower Cretaceous calcareous nannoplankton biostratigraphy. *Abh. Geol. B.–A.* 29, 3–52.

Thierstein H. 1975: Calcareous nannoplankton biostratigraphy at the Jurassic-Cretaceous boundary. Colloque sur la Limite Jurassique-Crétacé. *Bur. Rech. Geol. Minieres, Mem.*, 84–94.

Tremolada F., Bornemann A., Bralower T., Koeberl C. & van de Schootbrugge B. 2006: Paleoceanographic changes across the Jurassic/Cretaceous Boundary: the calcareous phytoplankton response. *Earth Planet. Sci. Lett.* 241, 361–371.

van de Schootbrugge B., Föllmi K.B., Bulot L.G. & Burns S.J. 2000: Paleoceanographic changes during the Early Cretaceous (Valanginian–Hauterivian): Evidence from oxygen and carbon stable isotope. *Earth Planet. Sci. Lett.* 181, 15–31.

Vašíček Z., Reháková D., Michalík J., Peterčáková M. & Halásová E. 1992: Ammonites, aptychi, nanno- and microplankton from the Lower Cretaceous Pieniny Formation in the "Kysuca Gate" near Žilina (Western Carpathian Klippen Belt, Kysuca Unit).

Západ. Karpaty Paleont. 16, 43–57.

Weissert H. 1989: C-isotope stratigraphy, a monitor of paleoenvironmental changes: A case study from the Early Cretaceous. *Surv. Geophys.* 10, 1–16.

Weissert H., McKenzie J.A. & Channell J.E.T. 1985: Natural variations in the carbon cycle during the Early Cretaceous. In: The carbon cycle and atmospheric CO_2: Natural variations Archean to the present. *Geophysic. Monograph.* 32, 531–545.

Wessely G. 2008: Kalkalpine Schichtfolgen und Strukturen im Wienerwald. *J. Alp. Geol.* 49, 201–214.

Appendix

Crossplot of the $\delta^{18}O$ vs. $\delta^{13}C$ values at Nutzhof (both vs. V-PDB).